SLAC-PUB-7147
BIHEP-EP1-96-02
April 1996

Measurement of the Pseudoscalar Decay Constant, f_{D^*}

J. Z. Bai,[1] O. Bardon,[6] I. Blum,[11] A. Breakstone,[9] T. Burnett,[12] G. P. Chen,[1] H. F. Chen,[4] J. Chen,[5] S. J. Chen,[1] S. M. Chen,[1] Y. Chen,[1] Y. B. Chen,[1] Y. Q. Chen,[1] B. S. Cheng,[1] R. F. Cowan,[6] , X. Z. Cui,[1] H. L. Ding,[1] Z. Z. Du,[1] W. Dunwoodie,[8] X. L. Fan,[1] J. Fang,[1] M. Fero,[6] C. S. Gao,[1] M. L. Gao,[1] S. Q. Gao,[1] P. Gratton,[11] J. H. Gu,[1] S. D. Gu,[1] W. X. Gu,[1] Y. F. Gu,[1] Y. N. Guo,[1] S. W. Han,[1] Y. Han,[1] F. A. Harris,[9] M. Hatanaka,[3] J. He,[1] M. He,[7] D. G. Hitlin,[3] G. Y. Hu,[1] T. Hu,[1] X. Q. Hu,[1] D. Q. Huang,[1] Y. Z. Huang,[1] J. M. Izen,[11] Q. P. Jia,[5] C. H. Jiang,[1] S. Jin,[1] Y. Jin,[1] L. Jones,[3] S. H. Kang,[1] Z. J. Ke,[1] M. H. Kelsey,[3] B. K. Kim,[11] D. Kong,[9], Y. F. Lai,[1] H. B. Lan,[1] P. F. Lang,[1] A. Lankford,[10] F. Li,[1] J. Li,[1] P. Q. Li,[1] Q. Li,[7] R. B. Li,[1] W. Li,[1] W. D. Li,[1] W. G. Li,[1] X. H. Li,[1] X. N. Li,[1] S. Z. Lin,[1] H. M. Liu,[1] J. H. Liu,[1] Q. Liu,[1] R. G. Liu,[1] Y. Liu,[1] Z. A. Liu,[1] X. C. Lou,[11] B. Lowery,[11] J. G. Lu,[1] S. Luo,[1] Y. Luo,[1] A. M. Ma,[1] E. C. Ma,[1] J. M. Ma,[1] H. S. Mao,[1] Z. P. Mao,[1] R. Malchow,[5] M. Mandelkern,[10] X. C. Meng,[1] H. L. Ni,[1] J. Nie,[1] S. L. Olsen,[9] J. Oyang,[3] D. Paluselli,[9] L. J. Pan,[9] J. Panetta,[3] F. Porter,[3] E. Prabhakar,[3] N. D. Qi,[1] Y. K. Que,[1] J. Quigley,[6] G. Rong,[1] M. Schernau,[10] B. Schmid,[10] J. Schultz,[10] Y. Y. Shao,[1] D. L. Shen,[1] H. Shen,[1] X. Y. Shen,[1] H. Y. Sheng,[1] H. Z. Shi,[1] X. R. Shi,[3] A. Smith,[10] E. Soderstrom,[8] X. F. Song,[1] J. Standifird,[11] D. Stoker,[10] F. Sun,[1] H. S. Sun,[1] S. J. Sun,[1] J. Synodinos,[8] Y. P. Tan,[1] S. Q. Tang,[1] W. Toki,[5] G. L. Tong,[1] E. Torrence,[6] F. Wang,[1] L. S. Wang,[1] L. Z. Wang,[1] M. Wang,[1] P. Wang,[1] P. L. Wang,[1] S. M. Wang,[1] T. J. Wang,[1] Y. Y. Wang,[1] C. L. Wei,[1] S. Whittaker,[2] R. Wilson,[5] W. J. Wisniewski,[13†] D. M. Xi,[1] X. M. Xia,[1] P. P. Xie,[1] D. Z. Xu,[1] R. S. Xu,[1] Z. Q. Xu,[1] S. T. Xue,[1] R. Yamamoto,[6] J. Yan,[1] W. G. Yan,[1] C. M. Yang,[1] C. Y. Yang,[1] W. Yang,[1] M. H. Ye,[1] S. Z. Ye,[1] K. Young,[12] C. S. Yu,[1] C. X. Yu,[1] Z. Q. Yu,[1] C. Z. Yuan,[1] B. Y. Zhang,[1] C. C. Zhang,[1] D. H. Zhang,[1] H. L. Zhang,[1] J. Zhang,[1] J. W. Zhang,[1] L. S. Zhang,[1] S. Q. Zhang,[1] Y. Zhang,[1] Y. Y. Zhang,[1] D. X. Zhao,[1] H. W. Zhao,[1] J. W. Zhao,[1] M. Zhao,[1] W. R. Zhao,[1] J. P. Zheng,[1] L. S. Zheng,[1] Z. P. Zheng,[1] G. P. Zhou,[1] H. S. Zhou,[1] L. Zhou,[1] X. F. Zhou,[1] Y. H. Zhou,[1] Q. M. Zhu,[1] Y. C. Zhu,[1] Y. S. Zhu,[1] B. A. Zhuang,[1] G. Zioulas[10]
(BES Collaboration)

[1] *Institute of High Energy Physics, Beijing 100039, People's Republic of China*
[2] *Boston University, Boston, Massachusetts 02215*
[3] *California Institute of Technology, Pasadena, California 91125*
[4] *China's University of Science and Technology, Hefei 230026, People's Republic of China*
[5] *Colorado State University, Fort Collins, Colorado 80523*
[6] *Massachusetts Institute of Technology, Cambridge, Massachusetts 02139*
[7] *Shandong University, Jinan 250100, People's Republic of China*
[8] *Stanford Linear Accelerator Center, Stanford, California 94309*
[9] *University of Hawai'i, Honolulu, Hawai'i 96822*
[10] *University of California at Irvine, Irvine, California 92717*

[11] *University of Texas at Dallas, Richardson, Texas 75083-0688*
[12] *University of Washington, Seattle, Washington 98195*
[13] *Superconducting Supercollider Laboratory, Dallas, Texas 75237-3946*

Abstract

Purely leptonic decays of the charged D meson have been studied using the reaction $e^+e^- \to D^{*+}D^-$ at a center of mass energy of 4.03 GeV. A search was performed for $D \to \mu\nu_\mu$ recoiling against a D^0 or D^+ which had been reconstructed from its hadronic decay products. A single event candidate was found in the reaction $e^+e^- \to D^{*+}D^-$, where $D^{*+} \to \pi^+ D^0$ with the $D^0 \to K^-\pi^+$, and the recoiling D^- decaying via $D^- \to \mu^-\bar{\nu}_\mu$. This yields a branching fraction value $B(D \to \mu\nu_\mu) = 0.08^{+0.16+0.05}_{-0.05-0.02}\,\%$, and a corresponding value of the pseudoscalar decay constant $f_D = 300^{+180+80}_{-150-40}$ MeV.

(Submitted to Physical Review D)

Typeset using REVTEX

*Work supported in part by the National Natural Science Foundation of China under Contract No. 19290400 and the Chinese Academy of Sciences under contract No. KJ85 (IHEP); by the Department of Energy under Contract Nos. DE-FG02-91ER40676 (Boston University), DE-FG03-92ER40701 (Caltech), DE-FG03-93ER40788 (Colorado State University), DE-AC02-76ER03069 (MIT), DE-AC03-76SF00515 (SLAC), DE-FG03-91ER40679 (UC Irvine), DE-FG03-94ER40833 (U Hawai'i), DE-FG05-92ER40736 (UT Dallas), DE-AC35-89ER40486 (SSC Lab); by the U.S. National Science Foundation, Grant No. PHY9203212 (University of Washington); and by the Texas National Research Laboratory Commission under Contract Nos. RGFY91B5, RGFY92B5 (Colorado State), and RCFY93-316H (UT Dallas).

†Present address: Stanford Linear Accelerator Center, Stanford, California 94309.

Purely leptonic decays of the D^+ [1] meson proceed via annihilation of the charm and anti-down quarks into a virtual *W* boson. The decay rate of this Cabbibo-suppressed process is determined by the wavefunction overlap of the two quarks at the origin, and is parametrized by the *D* meson decay constant, f_D. The leptonic decay width of the *D* can be written as [2]

$$\Gamma(D \to \ell\nu_\ell) = \frac{G_F^2|V_{cd}|^2}{8\pi} f_D^2 m_D m_\ell^2 (1 - \frac{m_\ell^2}{m_D^2})^2, \quad (1)$$

where G_F is the Fermi constant, V_{cd} is the $c \to d$ CKM matrix element [3], m_D is the mass of the D^+ meson, and m_ℓ is the lepton mass.

Theoretical models predict values of f_D and f_{D_s} (the D_s meson decay constant) which vary from 90 to 350 MeV [2,4–9]. The measurements of f_D and f_{D_s} have special relevance to theoretical calculations of f_B, whose value is of considerable importance to predictions of $B^0\overline{B^0}$ mixing [10]. However, the determination of f_B is very difficult, since the branching fraction for $B \to \mu\nu_\mu$ is expected to be very small. Hence information on leptonic decays of charmed mesons is very useful. To date, there are experimental measurements of f_{D_s} from the WA75 [11], CLEO [12] and BES [13] groups. For $D \to \mu\nu_\mu$, only a branching fraction upper limit of 0.07% (corresponding to $f_D \leq 290$ MeV at 90% C.L.) has been set by the Mark III Collaboration [14].

In this paper the results of a search for the Cabbibo-suppressed decay $D \to \mu\nu_\mu$ are reported. The data were collected using the Beijing Spectrometer at the Beijing e^+e^- Collider. A total integrated luminosity of 22.3 pb^{-1} was taken at cm. energy 4.03 GeV. At this energy $D^*\overline{D^*}$, $D^*\overline{D}$, $D\overline{D}$, and $D_S\overline{D_S}$ events are produced. The final states $D^{*0}\overline{D^{*0}}$ and $D^{*0}\overline{D^0}$ yield no D^+ mesons, since the decay $D^{*0} \to D^+\pi^-$ is cinematically forbidden. Also, the cross section values for D^+D^- and $D^{*+}D^{*-}$ production are much smaller than that for $D^{*+}D^-$ production. In addition, the $D^{*+}D^{*-}$ final state yields two undetected low momentum final state particles in addition to the two *D*'s, and this forces the missing mass squared variable used to define leptonic decay candidates into the region of semi-leptonic background (see below). For these reasons, the search for D^+ leptonic decay is restricted to the $D^{*+}D^-$ final state, which is characterized by D^+ mesons in the momentum range 370-650 MeV/c (taking into account the decay $D^{*+} \to D^+\gamma$, which has a branching fraction $\sim$1% [3]), or by D^0 mesons in the range 465-550 MeV/c. These regions are inaccessible to *D* mesons from the $D^*\overline{D^*}$ and $D\overline{D}$ final states.

Candidate $D^{*+}D^-$ events are defined by requiring that a D^0 or D^+, reconstructed from its hadronic decay products, have momentum in the appropriate range; this *D* meson is referred to as the tagging *D*. The system recoiling against the tagging *D* is then searched for the presence of a $D \to \mu\nu_\mu$ candidate. For such events, only the charged tracks from *D* decay and the recoil muon are fully reconstructed. A π^+ from D^{*+} decay has momentum less than 80 MeV/c, and is absorbed by the beampipe and inner wall of the central drift chamber. The existence of the ν_μ is inferred from the missing mass recoiling against the muon and the tagging *D*. This is small due to the neutrino mass, and the fact that the undetected pion or photon from D^{*+} decay has low momentum.

The Beijing Spectrometer is a solenoidal magnetic detector [15]. A four-layer central drift chamber (CDC) located just outside the beampipe is used in the event trigger. Each

charged track is reconstructed, and its energy loss measured, in a 40-layer main drift chamber (MDC) which covers 85% of the total solid angle. The momentum resolution is $1.7\%\sqrt{1+p^2}$ (p in GeV/c), and the dE/dx resolution is 11% for hadron tracks. An array of 48 barrel scintillation counters provides time-of-flight (TOF) measurement for charged tracks, with a resolution of 450 ps for hadrons. A 12-radiation-length, lead-gas barrel shower counter (BSC), operating in self-quenching streamer mode, measures the energies of electrons and photons over 80% of the total solid angle with an energy resolution of $22\%/\sqrt{E}$ (GeV). The solenoidal magnet provides a 0.4 T magnetic field in the central tracking region of the detector. Three double-layer muon counters instrument the magnet flux return, and serve to identify muons of momentum greater than 0.5 GeV/c. Endcap time-of-flight and shower counters extend coverage to the forward and backward regions.

The event trigger requires at least one barrel TOF hit within a time window of 40 ns, one hit in the outer two layers of the CDC and one charged track reconstructed by the on-line trigger logic using the hit pattern in the MDC, and a total energy in the BSC above 200 MeV.

The analysis begins with the selection of the tagging D decays. Two D^+ decay modes $(K^-\pi^+\pi^+, K^0_S\pi^+)$ and three D^0 decay modes $(K^-\pi^+, K^-\pi^+\pi^+\pi^-, K^0_S\pi^+\pi^-)$ have been considered, where $K^0_S \to \pi^+\pi^-$. Each charged track not from a K^0_S candidate was required to come from within 1 cm of the run-dependent interaction point in the transverse plane, and from within 15 cm along the beam direction. For each charged track, the polar angle (θ) had to satisfy $|\cos\theta| \leq 0.85$ in order that there be reliable tracking and barrel TOF information. The corresponding dE/dx and TOF measurements were required to be consistent with the mass hypothesis assigned to the track, and the kaon assignment further required $\chi^2_K < \chi^2_\pi$, where the χ^2 is the joint chi-squared of the available dE/dx and TOF information for the track in question. For the K^0_S, the $\pi^+\pi^-$ invariant mass was limited to 498 ± 30 MeV. The momentum of the tagging D was restricted to the range 440-620 MeV/c; for the $D^{*+}D^-$ final state, this is the interval corresponding to $D^* \to D\pi$ decay, extended at each end by twice the momentum resolution. This choice, together with particle identification requirements, serves almost to eliminate contamination from the $D_S{}^+ D_S{}^-$ final state at the small cost of reduced acceptance for $D^{*+} \to D^+\gamma$ decays. With this momentum requirement, the invariant mass distributions for the five tagging D decay modes are as shown in Fig. 1; in each case there is a signal indicating D production.

The number of $D^{*+}D^-$ events produced was extracted from the signal due to $D^+ \to K^-\pi^+\pi^+$ in Fig.1(a). A fit to this distribution yielded an estimate, N^{obs}, of 1409 ± 66 D^+ decays; the curve shown results from the fit. The number of $D^{*+}D^-$ events produced, N^{prod}, was then obtained from

$$N^{obs} = N^{prod} \times \varepsilon \times B(D^+ \to K^-\pi^+\pi^+) \times (1 + B(D^{*+} \to \pi^0 D^+) + B(D^{*+} \to \gamma D^+)) \quad (2)$$

where ε, the efficiency for reconstructing $D^+ \to K^-\pi^+\pi^+$, was found to be 22.6 ± 0.4 % from Monte Carlo simulation. This gave $N^{prod} \sim 52000$, and a cross section value $\sigma(e^+e^- \to D^{*+}D^-) = 2.33 \pm 0.23$ nb.

The events of Fig.1 containing a tagging D candidate were defined by requiring that the effective mass lie within three standard deviations of the relevant D mass [3]. The recoil system in each of these events was then checked for consistency with $D \to \mu\nu_\mu$ decay. It

was required that there be a single charged track with momentum between 700 and 1250 MeV/c having dE/dx, TOF and BSC information consistent with the muon hypothesis. This track was then extrapolated through the muon system, and was identified as a muon only if it had associated hits in at least two layers. For an event with a D^0 tagging mode, no isolated photons [16] were allowed to be present. However, an event with a D^+ tagging mode could have a low momentum photon or π^0 in addition to a recoiling D^-. Such an event was rejected if it had more than two isolated photons, or if it contained a photon having energy greater than 400 MeV. Only six muonic decay candidates survived these select ion procedures.

The scatter-plot of muon momentum versus missing mass squared recoiling against the muon and tagging D is shown in Fig.2 for the six candidate events. The contours at lower missing mass squared represent the region of the plot corresponding to the $D^{*+}D^-$ final state with one of the resulting *D's* decaying via the tagging mode, the other via $\mu\nu_\mu$. These contours were defined by means of Monte Carlo simulation [17], and thus take into account resolution effects.

To identify sources of background in the muonic decay data sample, 5×10^6 $D^{*+}D^-$ and 10^6 $D_s{}^+D_s{}^-$ events were generated by Monte Carlo simulation, and subjected to the selection criteria applied to the data. The D^{*+}, D^+, D^0, and D_S were allowed to decay according to their known branching fractions [3]. For all *D* tagging modes, the main background resulted from $D^{*+}D^-$ events in which one *D* did decay via the tagging mode, while the other decayed via $\pi K_L^0, \mu\nu_\mu K_L^0$, or $\mu\nu_\mu\pi^0$, with the K_L^0 or π^0 undetected. The contours at higher missing mass squared in Fig.2 were obtained, as for the lower missing mass squared contours, by simulating $D^{*+}D^-$ events in which one *D* decayed via a tagging mode, and the other via a mode which is a source of background.

The contours of Fig.2 indicate that, although the signal and background regions overlap substantially in muon momentum, they are quite well-separated in missing mass squared. Consequently, the signal region corresponding to $D \to \mu\nu_\mu$ is defined simply by requiring that the missing mass squared be less than 0.7 GeV^2. Only one event satisfies this further criterion. Its properties are listed in Table I, and the event display is shown in Fig.3. The event, which is tagged by the $D^0 \to K^-\pi^+$ mode, is very clean, with two hits in the muon system for the muon track, no extra photons, and K^- and π^+ tracks which are well-identified by dE/dx and the barrel TOF system. The π^+ from $D^{*+} \to D^0\pi^+$ is calculated to have a momentum $\sim$55 MeV/c; it should generate no hits in the CDC, and no hits are observed. The calculated momentum of the neutrino from $D^- \to \mu^-\overline{\nu_\mu}$ is $\sim$890 MeV/c, with polar angle $\sim$69 degrees, and azimuthal angle $\sim$ 164 degrees i.e. it passes through the BSC and muon system well within the fiducial volume; no BSC or muon counter activity should be generated in this region, and none is observed (cf. Fig.3). It follows that the event kinematics and the detector response are quite consistent with the interpretation of this event as being due to $e^+e^- \to D^{*+}D^-$, with $D^- \to \mu^-\overline{\nu_\mu}$.

For each tagging *D* mode, the expected background was estimated by Monte Carlo generation of 2×10^5 events for each of the contributing $\pi K_L^0, \mu\nu_\mu K_L^0$, and $\mu\nu_\mu\pi^0$ modes. The number of events satisfying the selection criteria and having missing mass squared less than 0.7 GeV^2 was then renormalizes to correspond to a luminosity of 22.3 pb^{-1}. The resulting background levels, which are listed in the fourth column of Table II, are all very small, and are consistent with the observation of only one event in the five tagging modes.

The corresponding Monte Carlo signal for missing mass squared greater than 0.7 GeV^2 is 5.2 events. In this region, an additional contribution is expected from $D \to \tau\nu_\tau$. Equation (1), together with the appropriate efficiency factor, would imply that for one $D \to \mu\nu_\mu$ event there should be ~ 0.3 event resulting from $D \to \tau\nu_\tau$ with $\tau \to \mu\nu_\mu\nu_\tau$. Such an event has three missing neutrinos, and so would fall in the background region of missing mass squared in Fig.2. It follows that the total number of background events expected is ~ 5.5, in good agreement with the 5 events observed.

In order to extract a value for the *D* muonic branching fraction, *B*, a likelihood function was constructed as the product of the Poisson probability functions for the individual tagging modes. For a D^+ tagging mode, *i*, the expected number of signal events is

$$\begin{aligned} N_i^{exp} &= 2N^{prod} \times (B(D^{*+} \to \pi^0 D^+) \\ &\quad + B(D^{*+} \to \gamma D^+)) \times B(D^+ \to i) \times \varepsilon_i \times B \\ &= C_i \times \varepsilon_i \times B, \end{aligned} \tag{3}$$

where N^{prod} is from equation (2); ε_i is the over all efficiency taking account of the muon, and the factor 2 occurs since either charged *D* can decay muonically. Similarly, for a D^0 tagging mode, *i*, the expected number of signal events is

$$\begin{aligned} N_i^{exp} &= N^{prod} \times B(D^{*+} \to \pi^+ D^0) \\ &\quad \times B(D^0 \to i) \times \varepsilon_i \times B \\ &= C_i \times \varepsilon_i \times B. \end{aligned} \tag{4}$$

In equations (3) and (4), C_i is the number of charged *D* mesons produced in association with tagging mode *i* (i.e. the number of non-tagging D^+), and is calculated using N^{obs} (the observed number of D^+ decays to $K^-\pi^+\pi^+$), ε, and the appropriate function of D^{*+} and *D* branching fractions (see equn. (2)). The values of the C_i and ε_i are listed in the second and third columns of Table II. The expected number of observed events in tagging mode *i* is then $(C_i \times \varepsilon_i \times B + bg_i)$, where bg_i is the expected number of background events, and the likelihood function is given by

$$L = exp(-B\Sigma_{i=1,5}(C_i \times \varepsilon_i)) \times (C_1 \times \varepsilon_1 \times B + bg_1), \tag{5}$$

where tagging mode 1 corresponds to $D^0 \to K^-\pi^+$; a factor $exp(-\Sigma_{i=1,5} bg_i)$ has been removed, since it does not depend on *B*. It should be noted that only the background estimate for tagging mode $D^0 \to K^-\pi^+$ appears in this function. The dependence of *L* on *B* is shown in Fig.4(a), and the maximum value occurs for

$$B = \frac{1}{\Sigma_{i=1,5}(C_i \times \varepsilon_i)} - \frac{bg_1}{C_1 \times \varepsilon_1}. \tag{6}$$

This gives $B = 0.08^{+0.16}_{-0.05}$ %, where the errors result from the values of *B* corresponding to 68.3% of the area under the curve above and below the maximum position (i.e. the unshaded area of Fig.4(a)).

The systematic errors on *B* are estimated from the uncertainties in the *D* and D^{*+} branching fractions [3], from the error on the number of D^+ decays to $K^-\pi^+\pi^+$, by varying

bg_1 by 50%, and, predominantly, by varying the event selection criteria, and thereby the efficiencies. The final result is

$$B(D \to \mu\nu) = 0.08^{+0.16+0.05}_{-0.05-0.02}\ \%, \tag{7}$$

where the second errors are systematic. From equation (1), with D^+ life-time 1.057 ps [3],

$$f_D{}^2 = 1.136 \times B, \tag{8}$$

with f_D in GeV and B in %. Substituting B in terms of f_D into equation (5), the dependence of the likelihood function on f_D is as shown in Fig.4(b). The procedure followed for B yields

$$f_D = 300^{+180+80}_{-150-40}\ \text{MeV}, \tag{9}$$

where the systematic errors have been obtained from those on B by using equation (8).

Although the uncertainties in the values of $B(D \to \mu\nu)$ and f_D obtained in this experiment are large, it should be emphasized that the analysis procedure is independent of measured luminosity and the $D^{+*}D^-$ cross section value, and does not require model-dependent assumptions. The result for $B(D \to \mu\nu)$ is consistent with the upper limit set by the Mark III experiment (which obtained no candidate events), while that for f_D is comparable to the values obtained for f_{D_S} in recent experiments, as expected theoretically.

We would like to thank the staffs of the BEPC accelerator and the Computing Center at the Institute of High Energy Physics (Beijing).

REFERENCES

[1] Throughout the paper, reference to a particular charge configuration implies reference to the charge conjugate configuration as well.

[2] See, for example, J. L. Rosner, Phys. Rev. **D42,** 3732 (1990); C. H. Chang and Y. Q. Chen, Phys. Rev. **D46,** 3845 (1992) and Phys. Rev. **D49,** 3399 (1994).

[3] L. Montanet *et al.* (Particle Data Group), *Review of Particle Properties,* Phys. Rev. **D50,** 1173 (1994).

[4] C. Bernard *et al.*, Phys. Rev. D38, 3540 (1988); M. B. Gavela *et al.*, Phys. Lett. **206B,** 113 (1988); T. A. DeGrandand R. D. Loft, Phys. Rev. **D38,** 954 (1988); D. S. Du, Phys. Rev. **D34,** 3428 (1986).

[5] J. G. Bian and T. Huang, Modern Phys. Lett. **8,** 635 (1993); C. Dominguez and N. Paver, Phys. Lett. **197B,** 423 (1987); S. Narison, Phys. Lett. **198B,** 104 (1987); M. A. Shifman, Ups. Fix. Nauk **151,** 193 (1987).

[6] H. Krasemann, Phys. Lett. **96B,** 397 (1980); M. Suzuki, Phys. Lett. **162B,** 391 (1985); S. N. Sinha, Phys. Lett. **178B,** 110 (1986); P. Cea *et al.*, Phys. Lett. **206B,** 691 (1988); P. Colangelo, G. Nardulli and M. Pietroni, Phys. Rev. **D43,** 3002 (1991).

[7] D. Bortoletto and S. Stone, Phys. Rev. Lett. **65,** 2951 (1990); J. L. Rosner, Phys. Rev. **D42,** 3732 (1990).

[8] E. V. Shuryak, Nucl. Phys. **B198,** 83 (1982); R. R. Mendel and H. D. Trottier, Phys. Lett. **B231,** 312 (1989); S. Capstick and S. Godfrey, Phys. Rev. **D41,** 2856 (1988).

[9] For a recent summary see J. Richman and P. Burchat, Rev. Mod. Phys. **67,** 893 (1995). Also see Note on the Pseudoscalar-Meson Decay Constant and Note on the D Meson Branching Fractions in [3] above.

[10] I. Claudio *et al.*, Phys. Rev. **D41,** 1522(1990); M. Witherell, "Charm Weak Decay", in Proceedings of the XVI International Symposium on Photon-Lepton Physics, Cornell University, Ithaca, New York, August, 1993.

[11] S. Aoki *et al.*, Progress of Theor. Phys. **89,** 131 (1993).

[12] D. Acosta *et al.*, Phys. Rev. **D49,** 5690 (1993); see CLEO CONF 95-22, June 29, 1995, for an updated measurement.

[13] J. Bai *et al.*, Phys. Rev. Lett. **74,** 4599 (1995).

[14] J. Adler *et al.*, Phys. Rev. Lett. **60,** 1375 (1988).

[15] J. Z. Bai *et al.*, Nucl. Instr. and Methods **A344,** 319 (1994); J. Z. Bai *et al.*, Phys. Rev. Lett. 69, 3021 (1992).

[16] An isolated photon is defined as an e.m. shower of energy > 60 MeV and separated by at least 18 degrees from the direction of the nearest charged track.

[17] In the simulation, 20000 $D^{*+}D^{-}$ events were generated for each tagging *D* mode, with the other *D* decaying to $\mu\nu_{\mu}$. The contours at lower missing mass squared in Fig.2 represent the superposition of the reconstructed events for each tagging mode which survive the muonic decay selection criteria.

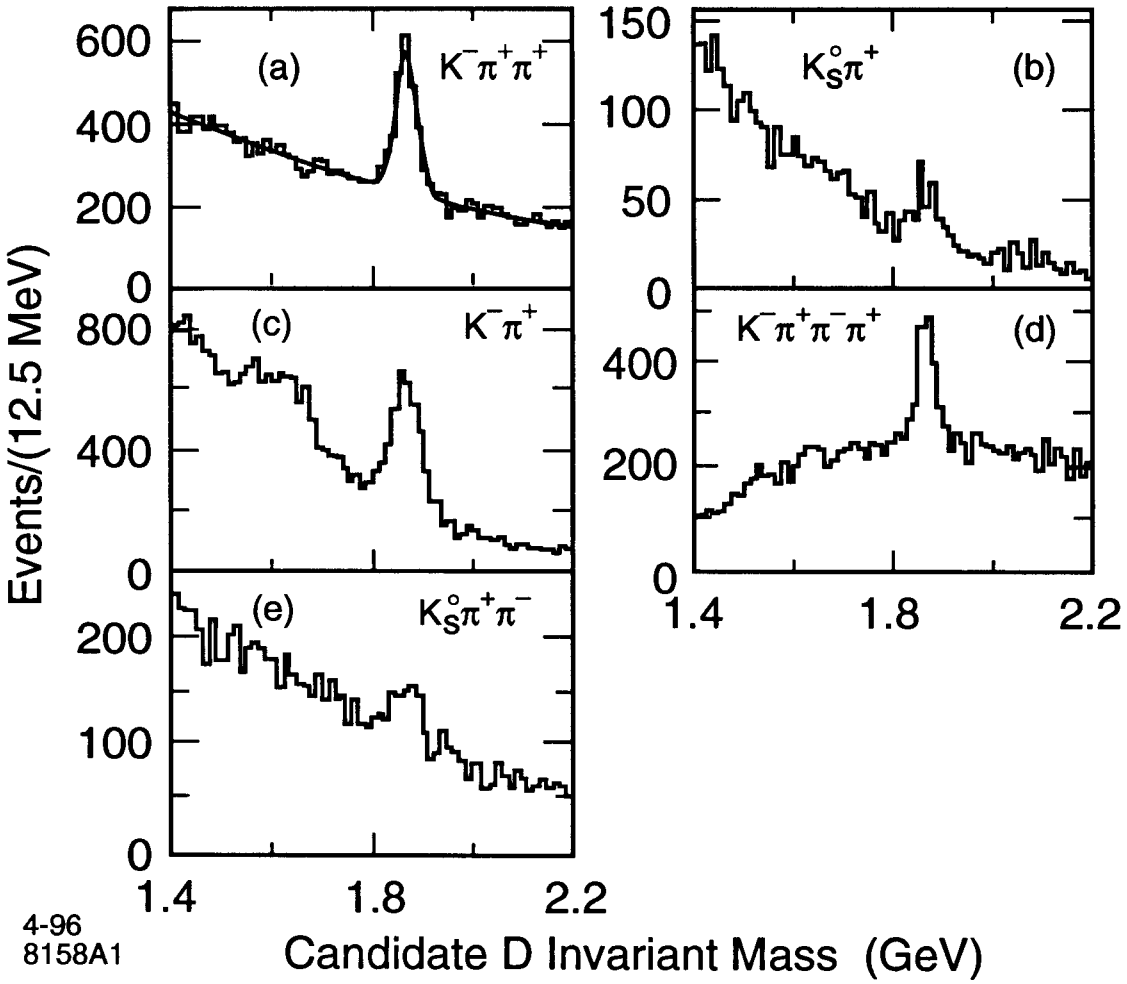

FIG. 1. The invariant mass distribution for the charged {(a),(b)} and neutral {(c),(d),(e)} *D* meson candidates selected as described in the text.

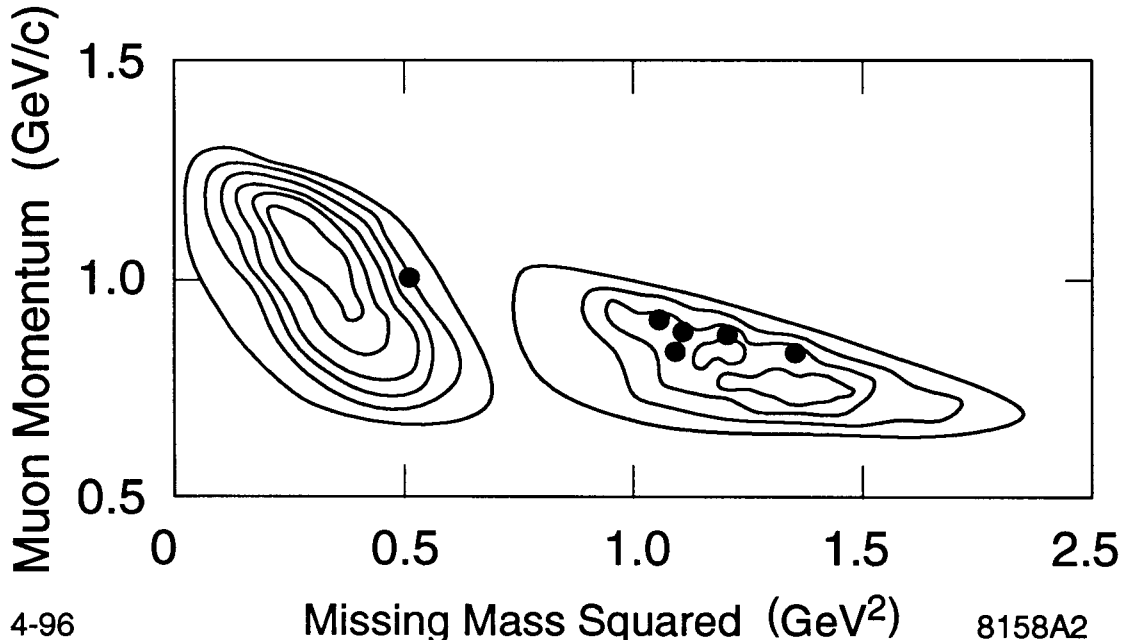

FIG. 2. The scatter-plot of muon momentum versus missing mass squared recoiling against the muon and tagging D for the surviving D muonic decay candidates (dots); the contours are described in the text.

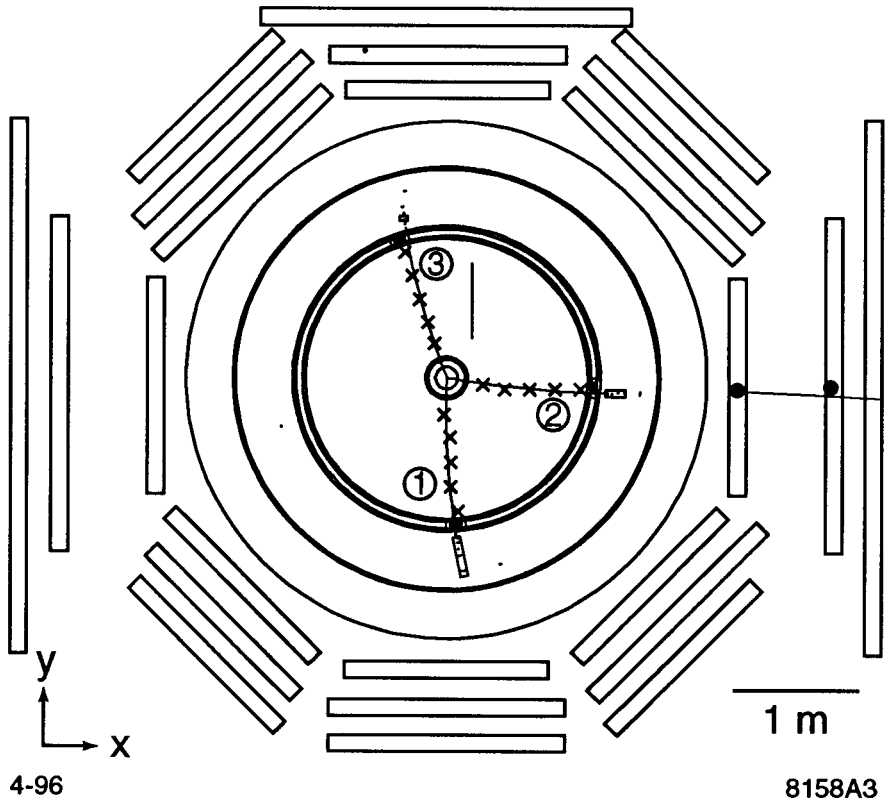

FIG. 3. The event display for the $D \to \mu\nu_\mu$ candidate; track 2 is the μ^-, and tracks 1 and 3 are the K^- and π^+ from D^0 decay, respectively.

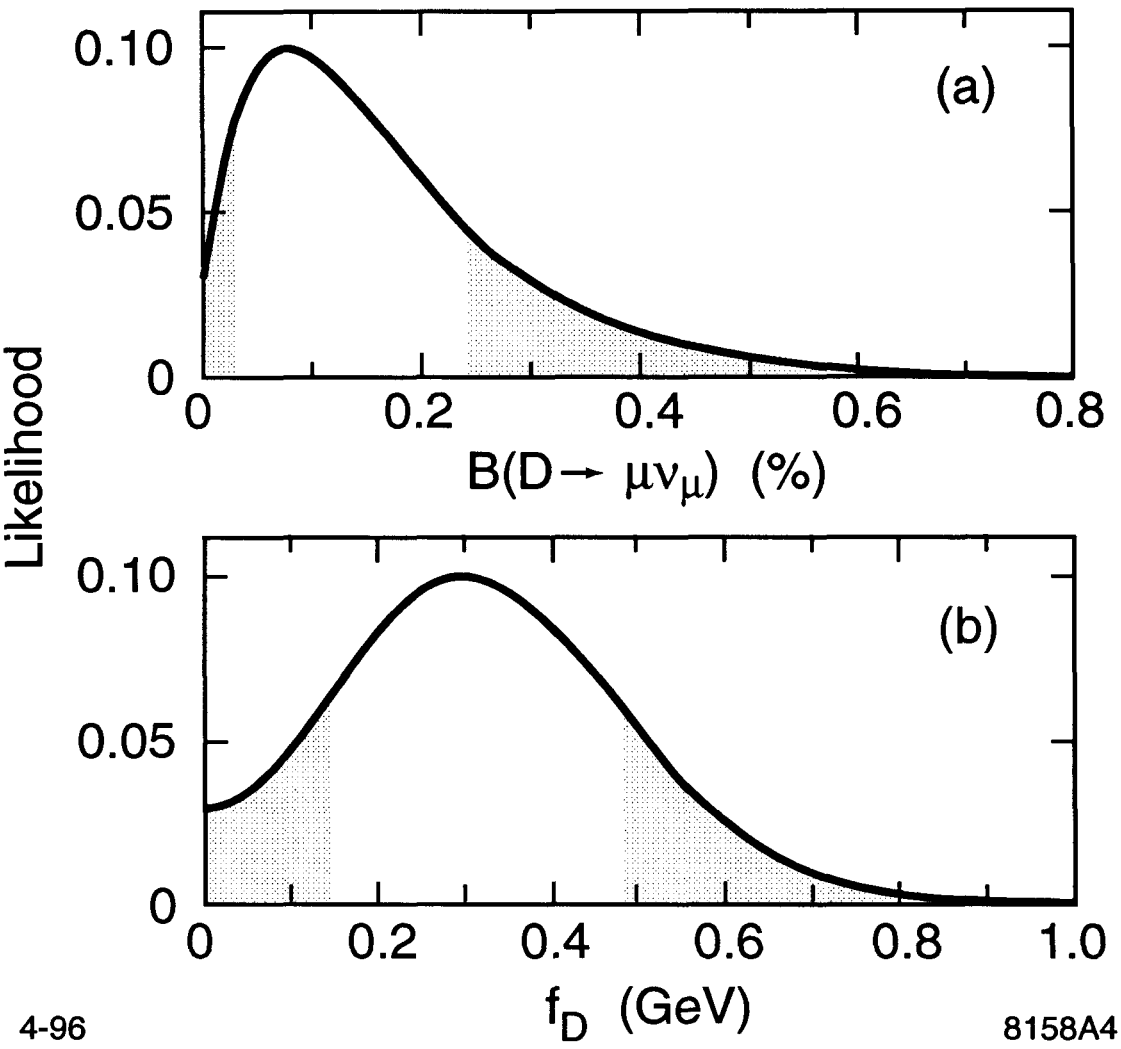

FIG. 4. The dependence of the likelihood function on (a) the value of the $D \to \mu\nu_\mu$ branching fraction, and (b) the value of f_D; the unshaded areas correspond to the one standard deviation errors described in the text.

TABLES

TABLE I. The properties of the D muonic decay candidate.

Tagging D Decay Mode	D^0 Mass (MeV)	Muon Momentum (MeV/c)	Missing Mass Squared (GeV^2)
$K^-\pi^+$	1850	1048	0.533

TABLE II. A summary of the data concerning the tagging D decay modes for the $D^{*+}D^-$ final state.

Tagging D Decay Mode	Number of Non-tagging D^+ (C_i)	Efficiency (ε_i) including μ (%)	Estimated Background (bg_i)
$K^-\pi^+$	1418	18.8 ± 0.3	0.03
$K^-\pi^+\pi^+\pi^-$	2865	9.5 ± 0.3	0.03
$K^0\pi^+\pi^-$	1875	3.2 ± 0.2	0.01
$K^-\pi^+\pi^+$	3016	15.6 ± 0.3	0.12
$K^0\pi^+$	908	5.5 ± 0.2	0.01
Total	10082		0.20